JOURNAL OF GEOPHYSICAL RESEARCH, VOL. 86, NO. C3, PAGES 1945–1953, MARCH 20, 1981

(12)

Satellite and Hydrographic Observations of Low-Frequency Wave Motions Associated With a Cold Core Gulf Stream Ring

THOMAS W. SPENCE

Department of Oceanography, Texas A&M University, College Station, Texas 77843

RICHARD LEGECKIS

National Environmental Satellite Service, Washington, D. C. 20233

Thermal infrared data from the NOAA polar orbiting satellite and hydrographic observations from surface ships are used to estimate the eccentricity and the rotation rate of wavelike perturbations around the circumference of a Gulf Stream cyclonic eddy in April 1977. From the satellite data, the rotation rate is estimated at $\omega = (4.4 \pm 0.1) \times 10^{-6}$ s^{-1} for the period April 8–16. Estimates of ω are obtained from the trajectory of satellite-tracked drifters and from changes in the sea surface temperature fields determined from expendable bathythermograph trace (XBT) surveys. A simple Eady model suggests the perturbations are stable modes of azimuthal wave number 2.

1. INTRODUCTION

Gulf Stream cyclonic rings are intense mesoscale features formed by meanders of the Gulf Stream. They are frequently observed to the east and south of the stream in the Sargasso Sea as cold, low-salinity anomalies. Recently, an interdisciplinary study of cyclonic rings by biological, chemical, and physical oceanographers was completed [*Backus et al.*, 1980]. The study focused on the evolution of such features by repeatedly observing them from the time of their formation until their demise.

During the study, one ring called BOB was formed from a meander, drifted westward as an isolated feature, interacted with the stream, reseparated, and drifted westward again until ultimately rejoining the stream near Cape Hatteras [*Doblar and Cheney*, 1977; *Backus et al.*, 1980; *Richardson*, 1980; *Vastano et al.*, 1980; *Watts and Olson*, 1978].

For a brief period between formation (Feburary 23) until interaction (April 20) the ring, an elliptical-shaped feature was observed in several infrared (IR) images obtained by the NOAA-5 very high resolution radiometer (VHRR) operated by the National Environmental Satellite Service, Washington, D. C. From the satellite data, one may estimate several aspects of the ring including its size, its shape, and certain subring scales of motion. Since remote observations of oceanic features from satellites are becoming more available, it is important to establish the connection between observed features and ocean dynamics. Thus we consider the implication of the satellite observations and complementary hydrographic observations in this study.

In particular, we present the evidence for rotation of subring scale perturbations from satellite and surface observations. From estimates of the relevant nondimensional parameters, we suggest that the elliptical shape is due to the presence of a stable wave with azimuthal wave number $n = 2$ [$\sim e^{in\theta}$] propagating around the circumference at a rotation rate about 20% of the maximum tangential velocity.

Paper number 80C1394.
0148-0227/81/080C-1394$01.00

2. OBSERVATIONS

Ring BOB was formed in late February from an intense meander. Fortunately, an excellent series of satellite infrared images was available to document its initial stages of development. Several details of the formation process have been presented elsewhere [*Doblar and Cheney*, 1977]. We have excerpted a selection of analyses made by the Naval Oceanographic Office for the period February 23, 1977, to April 20, 1977, which spans the time from formation until interaction with the Gulf Stream. In the sequence shown in Figure 1, the meander forms an isolated eddy which drifts slowly westward until it interacts with the stream. The interaction is extremely complex, but some aspects of it have been studied [*Glover*, 1977; *Janopaul*, 1979; *Richardson*, 1980; *Vastano et al.*, 1980].

After interaction, the eddy again separates and drifts in a clockwise trajectory toward Cape Hatteras. During this phase, the eddy was observed in detail on three separate cruises and was marked and followed with a satellite-tracked drifter. The postinteraction observations were discussed by *Backus et al.* [1980], *Olson* [1980], *Richardson* [1980], *Vastano et al.* [1980], and others. Here we are concerned with the earlier preinteraction period, however.

For the period shown in Figure 1, digital satellite data are available for two time intervals. These data were processed to remove geometric distortions according to an algorithm described by *Legeckis and Pritchard* [1976]. The resulting images were distortion free and could be used to estimate the shapes of the feature, an ellipse, and to estimate the eccentricity and orientation of the axes.

We made no correction for atmospheric attenuation. It would pose difficulty if it varied significantly over the scale of the ring, and if one were interested in quantitative surface temperature analyses. Neither is the case in our study. On March 9 and 12 the eddy appears as an isolated elliptical feature, and from April 8 to 16, there are five images showing the eddy first as an isolated elliptical feature, but later being encircled by Gulf Stream waters. Figure 2 shows two of the im-

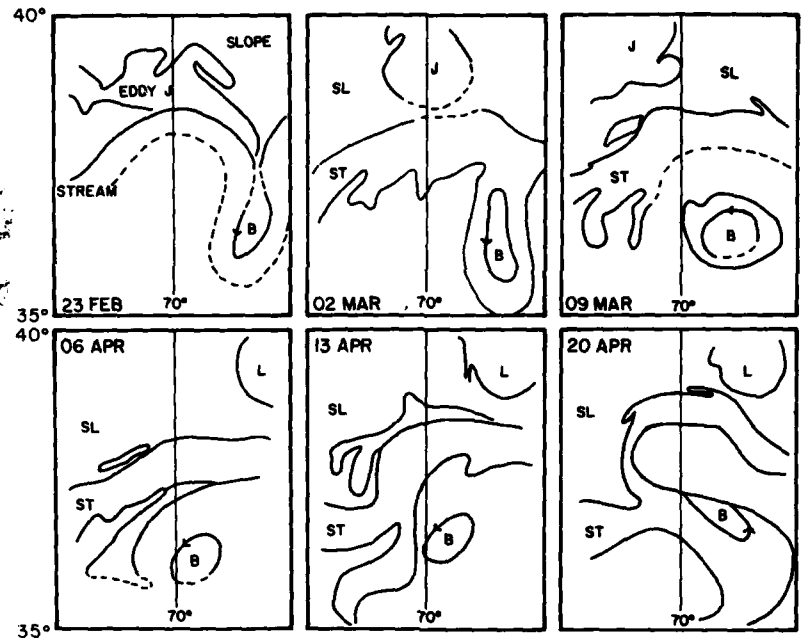

Fig. 1. Selected excerpts from the experimental frontal analysis [*U.S. Naval Oceanographic Office*, 1977] for the region of ring BOB showing the development, isolation, and interaction of the ring. B identifies ring BOB, J and L identify warm core rings. SL and ST are abbreviations of slope and Gulf Stream waters.

ages, and Figure 3 is a digital surface temperature field for the eddy region that corresponds to the outlined box in the two photographs. From the figures, a major and minor axis can be found, and the angular rotation rate of the axes can be calculated. We present data in Table 1 for the eccentricity ($\epsilon = (a^2 - b^2)^{1/2}/a$, where a, b are the semimajor and semiminor axes, respectively), the angle θ made by the major axis with east ($\theta > 0$ counterclockwise), and the rotation rate ω determined essentially by comparing the analyses at different times as illustrated in Figure 4. For convenience, we include $\omega' = \omega/f$ as a nondimensional rotation rate. Values are approximately 5% of $f = 2\Omega \sin \theta$. For the April data, several time intervals are available to estimate ω. From any single rectified photograph, the angle θ is likely to be determined to within about ±5°. Using that estimate, we find an error $\Delta\omega'$ of about ±10% for the 2- to 3-day averages, but for the interval April 8–16, only ±3%.

The April values are approximately the same as the earlier March one, suggesting that while isolated, the rotation rate of the axes may be about constant. The subsequent values show an increase of about 60% using the 2- and 3-day values through April 16. During this period, an unmistakable acceleration is occurring. When the shorter intervals are included, and when a less accurate image from April 19 is included, there is an apparent deceleration of approximately the same magnitude. Images from this later interval show the Gulf Stream to be encircling the ring, so our estimates suggest a 'spin-up' and 'spin-down' associated with the interaction process.

In addition to the satellite data, there are two types of observations which may also be used to obtain a rotation estimate. In April an extensive survey of the ring was carried out as part of the interdisciplinary ring study [*Schmitz et al.*, 1977]. R/V *Knorr* left Miami on April 9 en route to ring BOB. Upon arrival, a drifter was deployed, and an expendable bathythermograph trace (XBT) survey to determine the center and extent of the ring was made. Based on the center estimate, a detailed XBT star-shaped survey of the high-velocity region was made to determine the azimuthal structure of the ring [*Olson and Spence*, 1978]. These two portions of the cruise oc-

TABLE 1. Satellite Observations

Orbit	Time	θ, deg	ϵ	$\Delta\theta$, deg	Δt, day	$\omega \times 10^{-6}$ s^{-1}	$\omega' \times 10^{-2}$	$\Delta\omega'$	$R_T(T)$	$R_T(\rho)$
2764	12z March 9		0.72							
2796	02z March 12		0.84	58	2.5	4.68	5.46		0.26	
3130	14z April 8	125	0.83							
3167	14z April 11	171	0.68	46	3.0	3.10	3.61	0.4		
3192	14z April 13	211	0.73	40	2.0	4.04	4.71	0.58		
3198	02z April 14	226	0.77	15	0.5	6.06	7.07	2.35		
3229	14z April 16	288	0.91	62	2.5	5.01	5.84	0.47		
	April 19 (estimated)	330		42	3.0	2.8	3.3		0.20	0.26
Total	14z April 8 to 14z April 16			163	8	4.37	5.09	0.13		

cupied little more than 3 days, but we have divided the XBT's into two separate parts: April 14–15 (XBT's 90–141) and April 15–17 (XBT's 142–223).

Figure 5 shows the surface temperature field at the two times. From the second star-shaped array, a ring center was located at 36°42.0'N, 69°33.4'W. This value is within a few kilometers of independent center determinations made from subsurface estimates. It is also about where one would suggest from the satellite image based on locating the center of the area of an isotherm. For the time interval between the two analyses, we estimate $\omega' = 2 \times 10^{-2}$, and from the star survey, $\epsilon \simeq .9$, in reasonably good agreement with the satellite estimate.

The trajectory of the drifter launched in the ring (0731A) has been smoothed by a cubic spline and plotted by *Richardson* [1980, Figure 3*a*]. An eccentric orbit results, and from it we estimated the orientation of the major axes for a few intervals between launch date (April 14) and interaction (April 25). The data are shown in Table 2 and suggest a value for $\omega' \simeq 2.2 \times 10^{-2}$. In Figure 6 we plot the various ω' estimates.

Although there are some differences in the estimated values of ω' from the various observations, the sense and approximate magnitude of rotation is rather well established. The differences from the March to April satellite values are not significant from this small sample. The surface temperature and drifter estimates are smoothed over time and are likely biased toward lower values. The eccentricity apparently is decreasing for the ring when isolated, but increases during the interaction. These two observations suggest that the initial elliptic ring becomes more circular and that the axes rotate in the direction of mean flow.

In addition to the surface data presented above, there are other observations of the ring's interior fields. Corresponding to the mid-March period an XBT survey from R/V *Endeavor* [see *Richardson*, 1980, Figure 1*b*] and an AXBT survey [*Doblar*, 1977] were made. As noted above, extensive XBT and conductivity, temperature, and depth (CTD) data are available for the April period. From these sources, we may estimate the intensity of the ring and the magnitude of the azimuthal velocity component responsible for the rotation of the axes. For the XBT star-shaped survey, we may also decompose the temperature field into a mean radial variation and an azimuthal deviation from that mean [*Olson*, 1980; *Olson and Spence*, 1978]. The result of the (r, θ) decomposition is shown in Figure 7 for the star survey. All 83 XBT's were used to obtain a profile of the mean depth of the 15°C isotherm $\bar{Z}_{15}$ as a function of radial distance from the ring center. (*Olson* [1980, Figure 2] shows azimuthal mean depth for a selection of isotherms from later XBT observations of the ring.) On the figure, we analyze the depth anomaly field for each XBT, $\Delta Z_i = (\bar{Z}_{15} - Z_{15})_i$. Positive values mean that the 15°C isotherm was observed to be shallower than its average depth at its particular radial distance from center. Figure 7 suggests an azimuthal wave mode of the form $\phi = \phi(r, z)e^{i(n\theta - \omega t)}$ with $n = 2$.

The apparent rotation rate of the major-minor axis could be produced by the azimuthal circulation around the ring. One measure of the intensity of this circulation is the thermal Rossby number:

$$R_T = \frac{g\Delta\rho H}{\rho_0 f^2 L^2} = \frac{U_T}{fL}$$

where $\Delta\rho$ is the horizontal density difference, f the Coriolis parameter, H and L are characteristic vertical and horizontal dimensions, and U_T is the difference in azimuthal velocity from the bottom to the top of the layer. For the March XBT and AXBT surveys, only a rough value of R_T is available, but for the April period, CTD data and extensive XBT coverage permit a better estimate to be made. We show these values in Table 1, where $R_T(\rho)$ and $R_T(T)$ indicate the value is based on density or XBT data. Since salinity values are lower in the ring than in the surrounding water, the $R_T(T)$ value is an overestimate compared with the more accurate $R_T(\rho)$ value, but the latter is less representative of the ring since only one radial section of hydrographic stations is useful and $R_T(\rho)$ was available for only one time. Over 80 XBT's are included in the $R_T(T)$ value for the April case; about 20 for the March case.

One might expect a relationship similar to that observed in certain laboratory experiments with baroclinic flows. In these particular experiments, a cylindrical container is rotated about its axis at Ω with an imposed radial temperature gradient sufficiently strong to produce an elliptical ($n = 2$) wave which propagates steadily around the cylinder at rotation rate ω. (See *Spence and Fultz* [1977, Figure 1*b*], for example.) A series of 11 experiments at $\Omega = 0.22$ s^{-1} yields a least square regression of

$$\omega' = -0.001(\pm 0.001) + 0.263(\pm 0.023)R_T \text{ (standard error)}$$

The range of R_T was from 0.1 to 0.25. Using the R_T value of 0.26 from Table 1, one calculates a rate $\omega' = 0.067$, which is within 35% of the average satellite value of $\omega' = 0.05$. The laboratory experiments above are the continuously stratified, steady state analogs to the two-layer, transient experiments thought to be relevant to rings [*Saunders*, 1973].

TABLE 2. Drifter and Temperature Field Estimates

Time	$\Delta\theta$, deg	$\Delta\theta$, deg	$\omega \times 10^{-6}$ s^{-1}	$\omega' \times 10^{-2}$
Drifter Estimates (0731A, Richardson [1980])				
April 15–16	285			
April 18–19	315	30	2.0	2.36
April 21–22	352	37	2.49	2.91
April 24–25	370	18	1.21	1.41
Total		85	1.91	2.23
Temperature Field Estimate (Figure 5)				
April 14	278			
April 16–17	294	16	1.62	1.89

3. DISCUSSION

Analysis of the density fields of a series of cyclonic rings has shown them to be near-circular baroclinic vortices with azimuthal velocities which can be determined assuming a gradient balance [*Olson*, 1980]. Such vortices have been extensively studied in this and in other geophysical contexts, particularly with regard to their stability [*Charney*, 1973; *Saunders*, 1973; *Hart*, 1974; *Olson*, 1976].

Although the calculated velocity fields from cyclonic rings show a complex (r, z) dependence, it is useful to consider a simple representation to assess the stability of the flow to wavelike perturbations. Perhaps the simplest model to consider is due to *Eady* [1949]. We recast the model by consid-

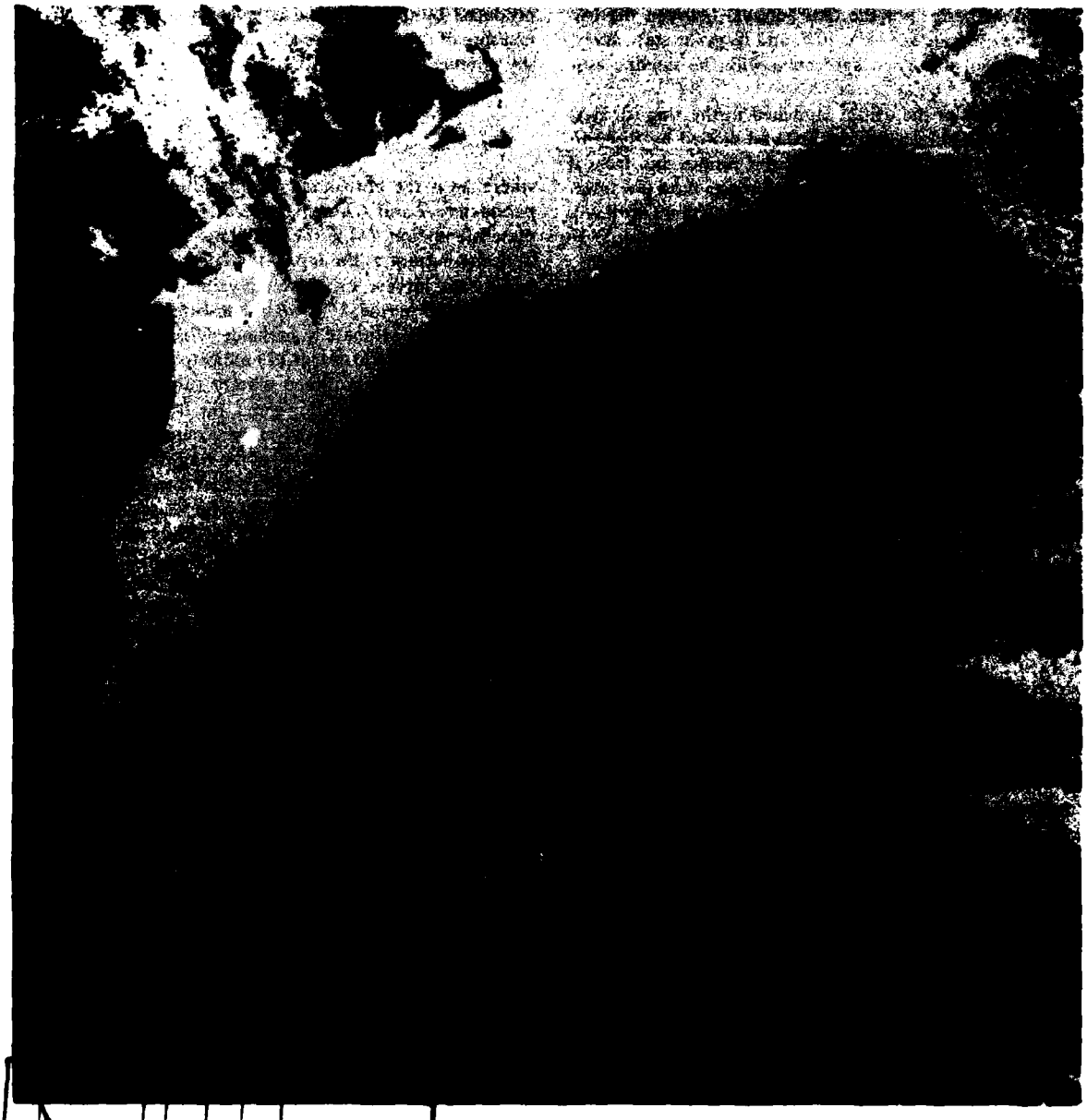

Fig. 2a

Fig. 2b

Fig. 2. The VHRR IR image of the Gulf Stream and eddies on (*a*) April 11, 1977, at 1400 GMT (NOAA-5 orbit 3167) and (*b*) April 13, 1977, at 1400 GMT (NOAA-5 orbit 3192). The image has been geometrically corrected to a universal transverse mercator map projection. The warmer water is represented by the darker shades of gray. The cyclonic eddy is enclosed by the box.

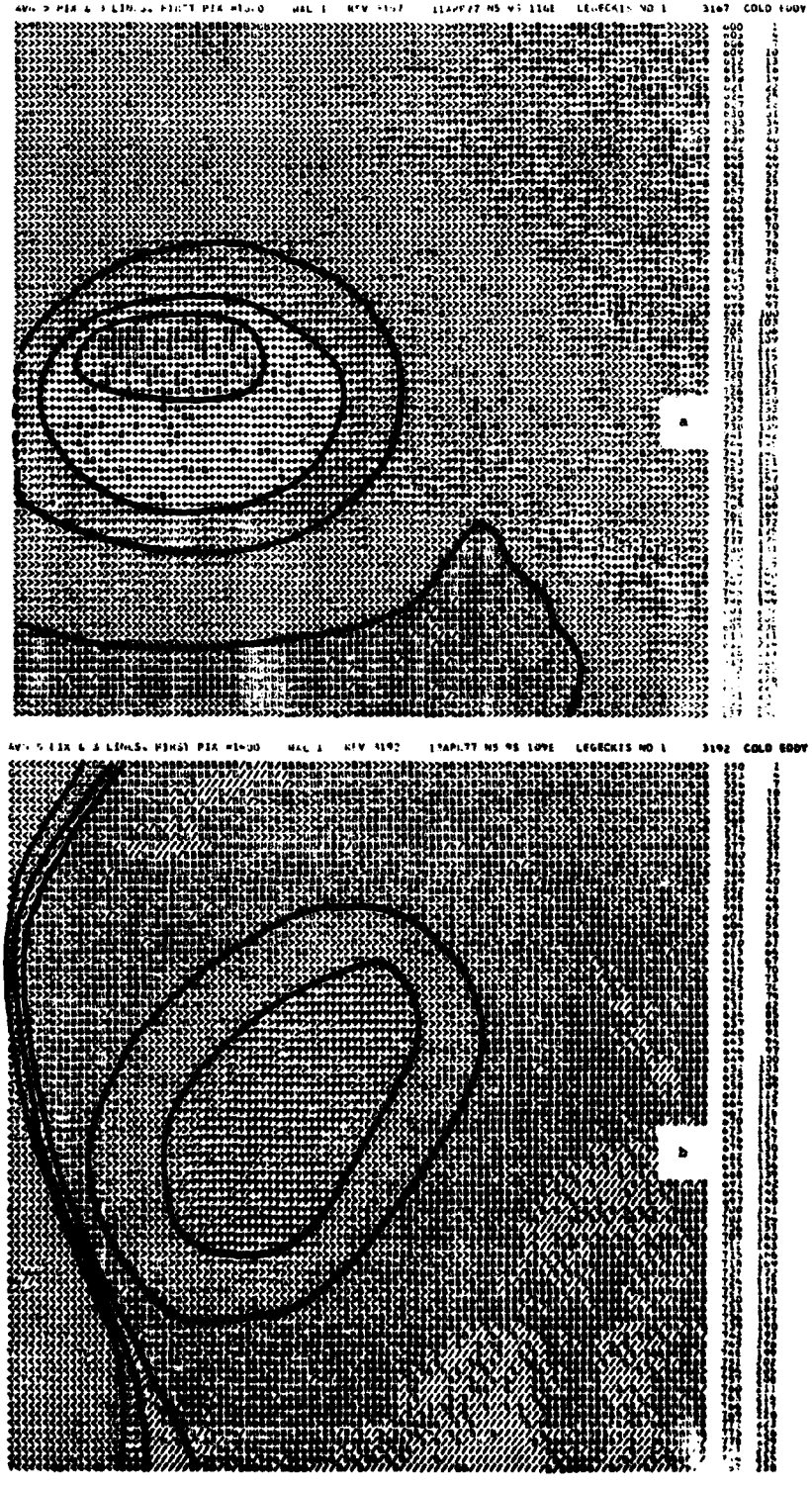

Fig. 3. The satellite radiometer temperatures for the area outlined by the box in Figures 2*a* and 2*b*. Each character represents a temperature value of a 2-km square.

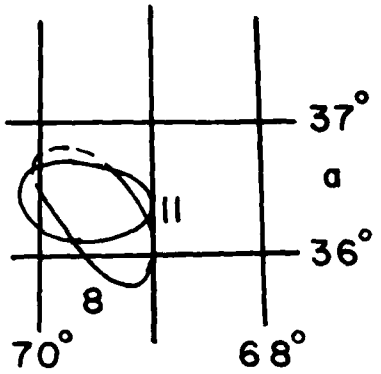

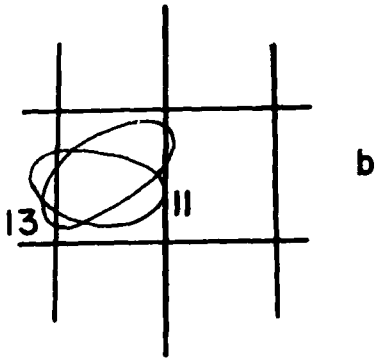

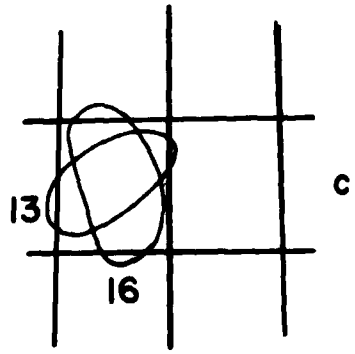

Fig. 4. A tracing of the eddy positions are shown for three intervals during April 1977. The eddy outline corresponds to the position of the maximum surface temperature gradient as observed from the satellite images.

ering the ring to be an inviscid baroclinic circular vortex with constant Brunt-Väisälä frequency,

$$N = \left(-\frac{g}{\rho_0}\frac{\partial \rho}{\partial z}\right)^{1/2}$$

on an f plane in which the basic state velocity field in (r, θ, z) is

$$\begin{aligned} v(r, z) &= (z + \tfrac{1}{2})r \qquad r \le 1 \\ v(r, z) &= (z + \tfrac{1}{2})/r \qquad r > 1 \end{aligned} \tag{1}$$

This flow excludes barotropic instability mechanisms, and with rigid boundaries at top and bottom, $z = \pm\frac{1}{2}$, yields a stability problem analogous to that of *Eady* [1949]. For a perturbation stream function of the form

$$\psi = \psi_0(z)e^{ik(n\theta - \omega Ct)}J_n(k_{n,s}r) \tag{2}$$

we obtain growing or decaying solutions for complex values of C, where

$$C = \frac{1}{2} \pm \left\{\frac{1}{4} + \frac{1}{\gamma^2} - \frac{\gamma \coth \gamma}{\gamma^2}\right\}^{1/2} \tag{3}$$

The bracketed quantity is negative for $\gamma = (NH/fL)k_{n,s} < \gamma_c = 2.39$, where $(NH/f) = L_D$, the Rossby radius of deformation [*Pedlosky*, 1979].

Recalling Figure 7, the largest displacement anomalies for the $n = 2$ mode are observed at a radius of about 50 km, which nearly coincides with the largest radial density gradient, i.e., the region of maximum v at $r = 1$. Consequently, if we specify that the perturbation radial dependence for this mode satisfies the condition

$$\frac{\partial}{\partial r}J_2(k_{1,s}r) = 0 \qquad r = 1 \tag{4}$$

we obtain $(NH/fL)^2 = B < B_c = (2.39/3.1)^2 = 0.58$ for instability. The observed vertical density gradient in the rings varies with r and z, but using averaged values, a mean of $N^2 \simeq 10^{-5}\ s^{-2}$ results. With $H/L \simeq (1500/50 \times 10^3) = 3 \times 10^{-2}$, we obtain a value of $B \simeq 1.2$. Thus for $n = 2$ the ring is apparently stable using this simple model.

4. Conclusions

In this paper we have used satellite infrared images of a Gulf Stream ring taken several days apart to show that the feature is elliptical with major-minor axes rotating counterclockwise at about 5% of f and 20% of U_T, the maximum velocity near the surface. In addition, based on surface measurements taken at the same time, we have obtained additional estimates of the eccentricity which agree well with the satellite values, and of the rotation rate which is somewhat lower, perhaps due to the longer times required to survey the feature in situ.

We suggest the elliptical shape is a wavelike perturbation of azimuthal mode 2, but based on an *Eady* [1949] type stability analysis, the wave appears to be stable. Since, in fact, the eccentricity was observed to decrease somewhat, the wave may be decaying in amplitude; a tendency toward more circular flow is physically plausible for rings isolated from the Gulf Stream.

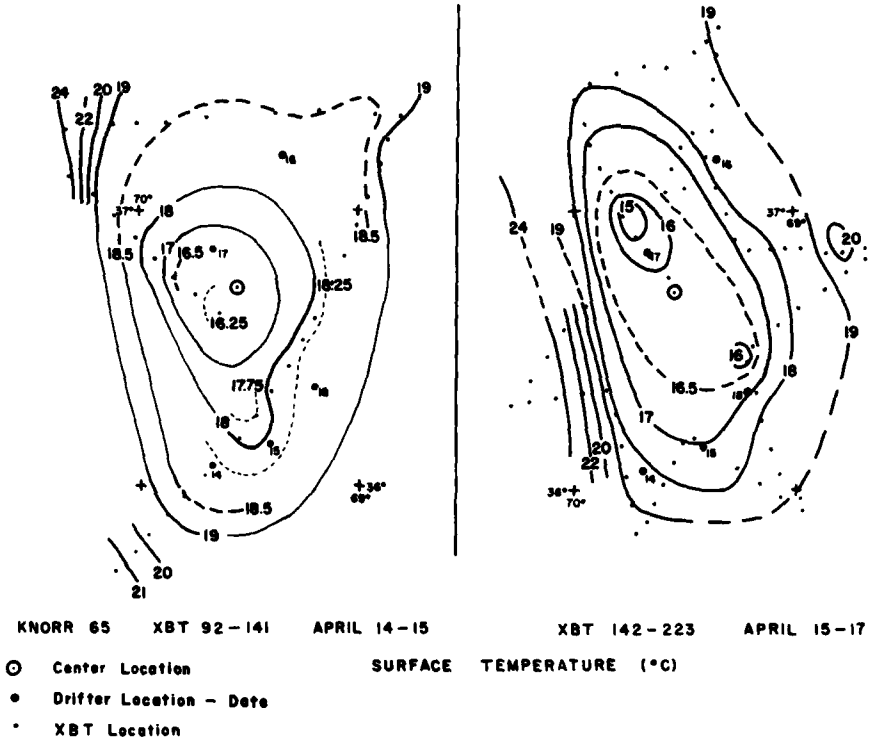

Fig. 5. Surface temperature analysis for (left) the period from *April 14 to 15* (XBT 90–141) and (right) the period from April 15 to 17 (XBT 142-223). The circled dot marks the center determined from April 15 to 17. The large solid dots mark the location (with date) of the drogued drifting buoy (0731A), and the small solid dots identify the XBT location.

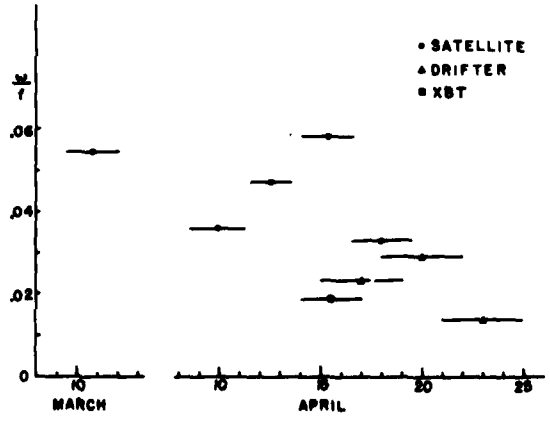

Fig. 6. Plot of observed nondimensional rotation rate $\omega' = \omega/f$ based upon satellite observations (solid dot), drifter observations (triangle), and XBT temperature observations (square). Horizontal lines show averaging periods.

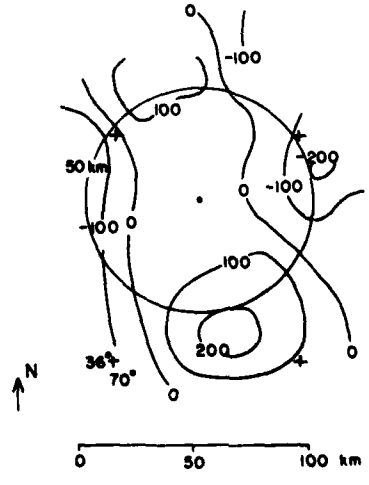

Fig. 7. An (r, θ) analysis of the depth anomaly of the 15°C isotherm $\Delta Z_{15} = (Z_{15} - \bar{Z}_{15})$, in meters for the star-shaped array (XBT 142–223).

Acknowledgments. The authors with to thank the participants of the Cold Core Ring Program for generously sharing their data. Support was provided in part by ONR contract N00014-75-C-0537.

REFERENCES

Backus, R. H., G. R. Flierl, D. R. Kester, D. B. Olson, P. L. Richardson, A. C. Vastano, P. H. Wiebe, and J. H. Wormth, Gulf stream ring physics, chemistry, and biology, submitted, 1980.

Charney, J. G., Planetary fluid dynamics, in *Dynamic Meteorology*, edited by P. Morel, D. Reidel, Hingham, Mass., 1973.

Doblar, R. A., Observations of a newly formed Gulf Stream ring, *Gulf Stream, 3*(3), 11, 1977.

Doblar, R. A., and R. E. Cheney, Observed formation of a Gulf Stream cold core ring, *J. Phys. Oceanogr., 7*, 944–946, 1977.

Eady, E. T., Long waves and cyclone waves, *Tellus, 1*, 1–33, 1949.

Glover, L. K., A wide body of warm water south of the stream, *Gulf Stream, 3*, 6–7, 1977.

Hart, J. E., On the mixed problem for quasi-geostrophic ocean currents, *J. Phys. Oceanogr., 4*, 349–356, 1974.

Janopaul, M. M., Water mass distribution in cyclonic rings, M.S. thesis, Tex. A&M Univ., College Station, 1979.

Legeckis, R., and J. Pritchard, Algorithm for correcting the VHRR imagery for geometric distortions due to the earth's curvature and rotation and roll attitude errors, *NOAA Tech. Memo, 77*, 1976.

Olson, D. B., Baroclinic instability and the spindown of a Gulf Stream ring, M.S. thesis, Tex. A&M Univ., College Station, 1976.

Olson, D. B., The physical oceanography of two rings observed by the cyclonic ring experiment, II, Dyamics, *J. Phys. Oceanogr., 10*, 514–528, 1980.

Olson, D. B., and T. W. Spence, Asymmetric disturbances in the frontal zone of a Gulf Stream ring, *J. Geophys. Res., 83*, 4691–4695, 1978.

Pedlosky, J., *Geophysical Fluid Dynamics*, Springer, New York, 1979.

Richardson, P. L., Gulf Stream ring trajectories, *J. Phys. Oceanogr., 10*, 90–104, 1980.

Saunders, P. M., The instability of a baroclinic vortex, *J. Phys. Oceanogr., 3*, 61–65, 1973.

Schmitz, J. E., D. E. Hagan, and A. C. Vastano, R/V *Knorr* cruise 65, *Phys. Oceanogr. Data Rep. II*, Tex. A&M Univ., 1977.

Spence, T. W., and D. Fultz, Experiments on wave-transition spectra and vacillation in an open rotating cyclinder, *J. Atmos. Sci., 34*, 1261–1285, 1977.

U.S. Naval Oceanographic Office, Experimental ocean frontal analysis charts, Washington, D. C., 1977.

Vastano, A. C., J. E. Schmitz, and D. E. Hagan, The physical oceanography of two rings observed by the cyclonic ring experiment, I, Physical structures, *J. Phys. Oceanogr., 10*, 493–513, 1980.

Watts, D. R., and D. B. Olson, Gulf Stream ring coalescence with the Gulf Stream off Cape Hatteras, *Science, 202*, 971–972, 1978.

(Received April 7, 1980;
revised September 29, 1980;
accepted September 30, 1980.)